Functional Nucleotide-Binding Domain in the F_oF_1-ATPsynthase α Subunit from the Yeast *Schizosaccharomyces pombe*†

Pierre Falson,*,‡ François Penin,§ Gilles Divita,‖ Jean-Pierre Lavergne,§ Attilio Di Pietro,§ Roger S. Goody,‖ and Danièle C. Gautheron⊥

Centre d'Etudes de SACLAY, Département de Biologie Cellulaire et Moléculaire, Section de Biophysique des Protéines et des Membranes, Unité de Recherche Associée 1290 du Centre National de la Recherche Scientifique, 91191 Gif sur Yvette Cedex, France, Institut de Biologie et Chimie des Protéines, Unité Propre de Recherche 412 du Centre National de la Recherche Scientifique, Campus de Gerland, 7 Passage du Vercors, 69367 Lyon Cedex, France, Max-Planck-Institut für Medizinische Forschung, Abteilung Biophysik, Jahnstrasse 29, 6900 Heidelberg, Germany, and Laboratoire de Biologie et Technologie des Membranes et des Systèmes Intégrés, Université Claude Bernard-Lyon I 43, Bd du 11 Novembre 1918, 69622 Villeurbanne Cedex, France

Received May 5, 1993; Revised Manuscript Received July 14, 1993⊛

ABSTRACT: The segment R_{165}–T_{330} of the α subunit of *Schizosaccharomyces pombe* F1-ATPase, corresponding to a putative nucleotide-binding domain by comparison with related nucleotide-binding proteins, has been overexpressed in *Escherichia coli*. Produced as a nonsoluble material, it was purified in a nonnative form, using a rapid procedure that includes one reversed-phase chromatography step. Refolding of the domain, called DNα19, was achieved quantitatively by using a high-dilution step and monitored by circular dichroism and intrinsic fluorescence. Once folded, DNα19 was highly soluble and stable. It bound 1 mol/mol either of adenine or guanine di- or triphosphate nucleotide, with a K_d ranging from 2.3 to 5.4 μM, or of methylanthraniloyl derivatives of the same nucleotides, with a K_d ranging from 0.2 to 0.6 μM. Interestingly, DNα19 was able to hydrolyze nucleoside triphosphates at a low but significant rate. The distance between one tryptophan residue located in the nucleotide-binding site and the ribose-linked methylanthraniloyl group of di- or triphosphate nucleotides was estimated by fluorescence resonance energy transfer to be 13 or 11 Å, respectively, suggesting that the tryptophan is close to the polyphosphate moiety of the nucleotide. This tryptophan residue was tentatively assigned to W_{190} by a hydrophobic cluster comparison with the H-*ras* p21 protein, suggesting that the putative loop of DNα19 containing W_{190} could play a functional role in nucleotide binding.

The F_oF_1-ATPsynthase[1] is a ubiquitous heterooligomeric protein inserted in bacterial, mitochondrial, or chloroplast membranes. The F_1 moiety of the complex is directly involved in ATP synthesis when associated to the membrane component, F_o, responsible for proton translocation. Once separated from F_o, F_1 becomes unable to synthesize ATP but gets a high ATPase activity and is therefore called F_1-ATPase. The stoichiometry of the F_1 moiety is $\alpha_3, \beta_3, \gamma, \delta, \epsilon$. The primary structure of each subunit is known for different organisms [for a review, see Walker *et al.* (1985)].

F_1 contains six nucleotide binding sites. Three of them are assumed to be catalytic and have a low selectivity for the adenine nucleotides. They are mainly borne by the β subunits [see for recent reviews Penefsky and Cross (1991), Allison *et al.* (1992), and Duncan and Cross (1992)]. The three others have a higher affinity and are quite specific for adenine nucleotides, although GTP has been reported to bind this type of site in the chloroplast F_1-ATPase (Guerrero *et al.*, 1990) and the mitochondrial F_1-ATPase associated with its natural protein inhibitor (Di Pietro *et al.*, 1988). They are mainly associated with the α subunits but are probably shared with the β subunits [(for reviews, see Allison *et al.* (1992) and Gromet-Elhanan (1992)]. The α and β subunits are organized in three $\alpha\beta$ pairs in which catalytic and noncatalytic sites are in close proximity (Vogel *et al.*, 1992; Zhuo *et al.*, 1992; Divita *et al.*, 1993b).

Besides the β subunit, which plays a major role in catalysis [for reviews, see Vignais and Lunardi, (1985), Futai *et al.* (1989), and Penefsky and Cross (1991)], the α subunit seems to have an important role, although this is less well documented. Isolated α subunits from *Escherichia coli* or rat liver mitochondria have been shown to bind adenine nucleotide or analogue (Dunn *et al.*, 1980; Lee *et al.*, 1990). Several bacterial mutants, having a single substitution in the sequence of the α subunit, were shown to have either low activity or defective assembly [Maggio *et al.*, 1987; Yohda *et al.*, 1988; for a review, see Senior (1988) and Futai *et al.* (1989)]. Using the F_1-ATPase from the yeast *Schizosaccharomyces pombe*, it was shown that the chemical modification of a single cysteine residue on one of the three α subunits and two on the γ subunit induces an almost complete inactivation of the enzyme,

† This work was supported by the CNRS-UMR 24, CNRS-UPR 412, and CNRS/MPG grants.

* Author to whom correspondence should be addressed.
‡ CNRS, Palaiseau.
§ CNRS, Lyon.
‖ Max-Planck-Institut.
⊥ Université Claude Bernard.

⊛ Abstract published in *Advance ACS Abstracts*, September 1, 1993.

[1] Abbreviations: F_oF_1, mitochondrial ATPase-ATPsynthase; F_1-ATPase, adenosine-5′-triphosphatase (EC 3.6.1.3); DNα19, chimerical polypeptide composed of the sequence MARIRA generated by the overexpression plasmid pT7-7 and the segment R_{165}–T_{330} of the ATPsynthase α subunit from the yeast *Schizosaccharomyces pombe*; NBD, nucleotide-binding domain; HPLC, high-pressure liquid chromatography; Mant-ATP, Mant-ADP, 3′*N*-methylanthraniloyladenosine 5′-tri/diphosphate; Mant-GTP, Mant-GDP, 3′-*N*-methylanthraniloylguanosine 5′-tri/diphosphate; Tris, 2-amino-2-(hydroxymethyl)-1,3-propanediol; EDTA, ethylenediaminetetraacetic acid; SDS, sodium dodecyl sulfate; SDS–PAGE, sodium dodecyl sulfate–polyacrylamide gel electrophoresis; PMSF, phenylmethanesulfonyl fluoride; Gdn-HCl, guanidine hydrochloride; DTT, dithiothreitol; TFA, trifluoroacetic acid; FRET, fluorescence resonance energy transfer; CD, circular dichroism.

0006-2960/93/0432-10387$04.00/0

decreases the nucleotide binding stoichiometry from 3 to 1 mol/mol of enzyme, and abolishes anion activation (Falson *et al.*, 1986). In addition, the F_1-ATPase of a mutant strain from this yeast was characterized by a loss of apparent negative cooperativity correlated to a decreased affinity for ADP and a lower amount of endogenous nucleotides (Falson *et al.*, 1987; Jault *et al.*, 1991). The identification of the mutation showed that the α subunit has the point substitution Q173L (Falson *et al.*, 1991) located in the first putative element of nucleotide binding of the subunit (Walker *et al.*, 1982). These results suggested that nucleotide binding to the α subunit was responsible for the apparent negative cooperativity of ATPase activity. The same conclusion was recently reached with the beef heart mitochondrial F_1-ATPase by Jault and Allison (1993), showing in addition that the apparent negative cooperativity was induced by the slow binding of ATP to a noncatalytic site. It was thus critical to characterize the capacity of the α subunit to interact with nucleotides to obtain more information on the regulation process. However, the whole α subunit of the yeast F_1-ATPase is not soluble once separated from the other subunits, as also observed for the pig heart mitochondrial enzyme (Gagliardi *et al.*, 1991), precluding such experiments. The work presented here shows that the latter difficulty was overcome by expressing in *E. coli* a segment from the α subunit corresponding to the nucleotide-binding domain. This approach was particularly successful since, after refolding, the polypeptide displays a high affinity for both adenine and guanine nucleotides or analogues and a low capacity to hydrolyze ATP or GTP. The comparison of the N-terminal parts of this segment with H-*ras* p21 suggests in addition that the domain adopts a β_1-L_1(P loop)-α_1-L_2-β_2 conformation, similar to that of H-*ras* p21.

MATERIALS AND METHODS

Reagents. [γ-^{32}P]ATP (3000 Ci/mmol) and [α-^{32}P]ATP (800 Ci/mmol) were from NEN and [γ-^{32}P]GTP (5000 Ci/mmol) and [^{35}S]dATPαS (1000 Ci/mmol) from Amersham. Unlabeled ATP, ADP, GTP, and GDP were from Boehringer Mannheim. The purity of the nucleotides was controlled by HPLC with a Partisil PXS (10–25) SAX column from Whatman as described by Falson *et al.* (1987). Acetonitrile was from Baker. All other products were obtained from Sigma in the highest purity available. *N*-Methylanthraniloyl derivatives of ADP, ATP, GDP, and GTP were prepared as described by John *et al.* (1990).

Enzymes, Plasmids, and Strains. T4 DNA ligase and the corresponding buffer, restriction enzymes, and IPTG were from Boehringer Mannheim. Sequenase 2.0 sequencing kit and plasmid pTZ18U were provided by the United States Biochemical Corp. Thermostable *Taq* DNA polymerase and the corresponding buffer were from Promega. Purified synthetic oligonucleotides were obtained from Appligene. Deoxynucleoside triphosphates (dATP, dGTP, dCTP, dTTP) were obtained from Pharmacia. Plasmids pT7-7 and pGP1-2 were generously given by Dr. S. Tabor. They were used in the *E. coli* strains DH1 (*rec*A1, *end*A1, *gyr*96, *thi*-1, *hsd*R17, *sup*E44) and K38 (Hfrλ), respectively, as described by Tabor (1990). The plasmid pTZ18U/ATP1 containing *Atp*1, the gene encoding the α subunit of the ATPsynthase from the yeast *S. pombe*, was described previously (Falson *et al.*, 1991).

Construction of the Overexpression Vector. Most recombinant DNA methods used were as described by Sambrook *et al.* (1989). A fragment of 517 bp, designated DNATP1, was amplified by the polymerase chain reaction (Mullis & Faloona, 1987), using the plasmid pTZ18U/ATP1 as template and the oligonucleotides 5′-CGGGATCCCGTGAGCTTATTATTGG-3′ and 5′-TCACAAGCTTAAGTTTCGATAAC-3′. The oligonucleotides were designed to amplify the region 1024–1516 of *Atp*1 and to introduce at the 5′- and 3′- ends of the amplified fragment respectively, *Bam*HI and *Hin*dIII restriction sites (mismatched bases are underlined). Amplification was carried out in 100 μL of 10 mM Tris-HCl, pH 9.0, 50 mM KCl, 1.5 mM $MgCl_2$, 0.1% Triton X-100, 20 μg/mL gelatin, 0.5 μM primers, 0.2 mM dNTPs, 2.5 units of *Taq* DNA polymerase, and 10^8 copies of the DNA template. The sample was submitted to a first thermal cycle of 2 min at 94 °C, 0.5 min at 45 °C, and 0.5 min at 72 °C, followed by 5 cycles of 0.5 min at 94 °C, 0.5 min at 45 °C (taking into account the mismatches), and 0.5 min at 72 °C, and then 25 cycles of 0.5 min at 94 °C, 0.5 min at 60 °C, and 0.5 min at 72 °C. During the last cycle, the extension step was prolonged to 5 min. After restriction with *Bam*HI and *Hin*dIII, the amplified DNA was inserted in the corresponding sites of pT7-7. The resulting plasmid pT7-7/DNATP1 was used to transform the *E. coli* strain DH1. Positive clones were selected by restriction analysis. The accuracy of both construction and DNA amplification was verified by dsDNA sequencing.

pT7-7/DNATP1 was used to transform the *E. coli* strain K38 containing the plasmid pGP1-2. The two-plasmid system was used as described by Tabor (1990). The expression of the protein was optimized by varying duration and temperature of induction. For this purpose, minicultures were performed in 1.0 mL of LB medium supplemented with antibiotics. Bacteria were then pelleted and dissolved in a cracking buffer (60 mM Tris-HCl, pH 6.8, 0.6 M 2-mercaptoethanol, 1% SDS, 10% glycerol, 0.01% Bromophenol Blue), and their protein content was analyzed by SDS–PAGE (Laemmli, 1970).

Expression and Purification of the Recombinant Protein. Six hundred milliliters of LB medium containing 50 μg of ampicillin/mL and 75 μg of kanamycin/mL was inoculated with 60 mL of an overnight culture of K38 containing pT7-7/DNATP1 and pGP1-2. The bacteria growth was carried out for 2 h at 30 °C. Expression was induced by increasing the temperature to 42 °C for 0.5 h and followed by an incubation during 1.5 h at 37 °C. The bacteria were harvested by low-speed centrifugation, washed twice with sterilized water to give 2–3 g of bacterial paste, which was aliquoted as 200-mg fractions in Eppendorf tubes, and stored in liquid nitrogen.

Two hundred milligrams of bacteria paste was homogenized with 0.8 mL of buffer A (0.1 M Tris-HCl, pH 8.0, 5 mM EDTA, 2% sodium deoxycholate, 1 mM NaN_3, 1 mM PMSF) in an Eppendorf tube and sonicated in ice for 30 s at 40 W with a small probe on a Branson sonifier. The suspension was centrifuged at 20000*g* for 20 min at 4 °C. The resulting pellet was suspended in 0.9 mL of buffer B (0.1 M Tris-HCl, pH 8.0, 5 mM EDTA, 1% Triton X-100, 2 M NaCl, 1 mM NaN_3, 1 mM PMSF), sonicated, and centrifuged as above. The pellet was suspended in 0.9 mL of buffer C (0.1 M Tris-HCl, pH 8.0, 5 mM EDTA, 1 mM NaN_3, 1 mM PMSF), sonicated, and centrifuged as above.

The pellet of inclusion bodies was homogenized in 0.9 mL of buffer D (0.1 M Tris-HCl, pH 8.0, 5 mM EDTA, 3 M Gdn-HCl, 5 mM DTT, 1 mM NaN_3, 1 mM PMSF) and incubated for 1 h at 20 °C. After centrifugation at 100000*g* for 30 min at 20 °C, the supernatant was diluted at room temperature under continuous stirring in 5 mL of buffer E (0.1 M Tris-HCl, pH 8.0, 5 mM EDTA, 5 mM DTT, 1 mM NaN_3, 1 mM PMSF). After dilution, the protein content flocculated in about 15 min, and the suspension was centrifuged at 20000*g* for 20 min at 15 °C. The pellet containing DNα19 was washed twice in sterilized water, using a mild sonication

to homogenize the solution, and centrifuged again at 20000g for 15 min at 15 °C. The progressive solubilization of the pellet was achieved by several successive steps of a mild sonication in 0.2 mL of 0.1% TFA, followed by a centrifugation in an Eppendorf centrifuge for 10 min at 15 °C. The supernatants were pooled and either stored in liquid nitrogen or immediately submitted to the reversed-phase HPLC step.

The HPLC was performed on a Waters apparatus consisting of two M510 pumps, a U6K injector, and a 990 photodiode array detector. Preparative chromatography was performed with a Radial PAK C4 cartridge (300 Å, 15 μm, 8 × 100 mm from Waters) equilibrated in 0.1% TFA and 15% acetonitrile. After the protein solution was loaded, the elution was carried out at a flow rate of 2 mL/min, using the following multislope linear gradient of acetonitrile in 0.1% TFA: (1) 15–24% in 6 min; (2) 24–25% in 10 min; (3) 25–38% in 5 min; (4) 38–60% in 11 min. Fractions containing DNα19 were pooled, lyophilized, solubilized in a small volume of 0.1% TFA, and then submitted to the same chromatographic step. After lyophilization, the protein was solubilized in 0.1% TFA, aliquoted as 300 μg/100 μL fractions, and stored in liquid nitrogen.

Refolding of DNα19. Six hundred micrograms of DNα19 (in 200 μL of 0.1% TFA) were lyophylized, dissolved in 600 μL of water, and then rapidly diluted under stirring in 20 mL of buffer F [25 mM Mes, pH 5.0 (Tris), 25 mM NaCl, 5 mM $MgCl_2$, 1 mM 2-mercaptoethanol]. After 1 h at 25 °C, the protein solution was concentrated to 20–80 μM by using a Centriprep concentrator equipped with a YM10 ultrafiltration membrane (Amicon) and then stored in liquid nitrogen. Before use, the solution was thawed at 25 °C, diluted to the needed concentration (typically 2 μM) in buffer G [25 mM Mes, pH 5.0 (Tris), 25 mM NaCl, 1 mM $MgCl_2$, 1 mM 2-mercaptoethanol], and equilibrated for at least 8 h.

Fluorescence Emission Measurements. Fluorescence experiments were performed with a SLM 8000 spectrofluorometer (SLM Aminco), with spectral bandwidths of 2 and 8 nm, respectively, for excitation and emission. The sample routinely contained 2 μM DNα19 in 0.6 or 1 mL of buffer G at 25 ± 0.1 °C. All measurements were corrected for the wavelength dependence of the exciting light intensity through the use of the quantum counter Rhodamine B in the reference channel (Lackowicz, 1983). The spectra were corrected for the background intensity of buffer fluorescence and for dilution effect (never exceeding 5%). The Raman scatter contribution was removed by subtraction of a buffer blank.

Emission spectra of the intrinsic tryptophan fluorescence were recorded between 305 and 460 nm upon excitation at 295 nm. The quenching of fluorescence induced by nucleotide binding was studied by following the decrease in fluorescence intensity between 310 and 380 nm in the presence of increasing amounts of nucleotides. A quartz cuvette with a 5-mm optical path length was used to minimize the inner-filter effect of the nucleotides. When necessary, measurements were corrected for the nucleotide inner effect by assaying a solution of 4 μM *N*-acetyltryptophanamide under the same conditions.

Extrinsic fluorescence emission spectra of the Mant-derivatized nucleotides were scanned from 370 to 650 nm. The excitation wavelength was 355 nm. The binding of nucleotide analogues was determined by monitoring the increasing fluorescence emission at 450 nm (John *et al.*, 1990).

Equation 1 was used to determine the K_d

$$F = F_{Ci} - \{(Et + L + K_d) - [(Et + L + K_d)^2 - 4EtL]^{1/2}\}(F_{Ci} - F_{Cf})/(2Et) \quad (1)$$

where F is the relative fluorescence intensity, F_{Ci} is the relative fluorescence intensity at the beginning of the titration, F_{Cf} is the fluorescence intensity at saturating concentration of ligand L, Et is the concentration of DNα19, and K_d is the dissociation constant of the DNα19–ligand complex. The fitting of the curve was accomplished on a computer with Grafit from Erithacus Software.

The distance between a tryptophan residue and the Mant derivative was measured spectroscopically by Förster energy transfer (Stryer, 1978; Lackowicz, 1983). The resonance energy-transfer efficiency E was determined by following either the decrease in the donor fluorescence, assuming that the local environment of the tryptophan residue is not changed by the binding of the acceptor to the protein (method 1), or the increase in the acceptor fluorescence, which takes into account a modification of the local environment of the donor due to the binding of the acceptor (method 2).

In method 1, the fluorescence intensity of the tryptophan residue is measured in the presence (F_{Da}) and in the absence (F_D) of the fluorescent nucleotide. E_1 is thus given by

$$E_1 = 1 - F_{Da}/F_D \quad (2)$$

In method 2, the increase of fluorescence at the acceptor excitation, induced by energy transfer from the tryptophan excited at 295 nm, is used to calculate E_2

$$E_2 = [F_{295}/F_{350} - \epsilon_{A295}/\epsilon_{A350}]\epsilon_{A350}/\epsilon_{D295} \quad (3)$$

where F_{295} and F_{350} are the corrected intensities of the excitation spectrum, ϵ_{A295} (2.85×10^3 M^{-1} cm^{-1}) and ϵ_{A350} (6.66×10^3 M^{-1} cm^{-1}) are the absorption coefficients of the Mant-nucleotide at 295 and 350 nm, and ϵ_{D295} (1.72×10^4 M^{-1} cm^{-1}) is the extinction coefficient of the protein at 295 nm.

The distance R between the fluorophores is given by

$$R = R_0(E^{-1} - 1)^{1/6} \quad (4)$$

where R is calculated in angstroms and R_0 is the Förster critical distance that gives 50% of the transfer efficiency (Förster, 1948). R_0 is calculated by (Stryer & Haugland, 1967)

$$R_0 = 9.79 \times 10^3(k^2 J \Phi_D \eta^{-4})^{1/6} \quad (5)$$

where η is the refractive index of the buffer ($\eta = 1.4$), Φ_D is the quantum yield of the donor (see after), k^2 is a factor of orientation for which a value of two-thirds can be used (Etfink, 1991), and J is the overlap integral in cm^3 M^{-1} given by (Fairclough & Cantor, 1978)

$$J = \int F_D(\lambda)\epsilon_A(\lambda)\lambda^4 d\lambda / \int F_D(\lambda)d\lambda \quad (6)$$

J is numerically integrated at 1-nm intervals, λ is the wavelength in centimeters, $F_D(\lambda)$ is the corrected fluorescence of the unquenched donor, and $\epsilon_A(\lambda)$ is the acceptor absorption coefficient in M^{-1} cm^{-1}. The maximal uncertainty in the calculated distance is likely to be less than ±10%.

The quantum yield Φ_D was determined to be 0.081 for tryptophan residues, on the basis of the value of 0.13 for *N*-acetyl-L-tryptophanamide (Chen, 1967) and

$$\Phi_D = \Phi_{st}([F_{295}/F_{295\text{-st}}][A_{295\text{-st}}/A_{295}]) \quad (7)$$

where Φ_D is the quantum yield of tryptophan residues in DNα19, Φ_{st} is the quantum yield of the standard, and F_{295} and $F_{295\text{-st}}$ are the areas of the emission spectrum of protein and standard, respectively, when excited at 295 nm. A_{295} and $A_{295\text{-st}}$ are the absorptions at 295 nm for DNα19 and the standard, respectively.

Circular Dichroism Measurements. CD spectra were collected on a Jobin-Yvon Mark IV dichrograph, at a constant

rate of 1 nm/min using a 0.02-cm path length cell. Protein samples were prepared as described above, at a concentration of 2 μM in buffer G, with or without 2 μM ATP and with or without 6 M Gdn-HCl. They were scanned from 190 to 260 nm, at room temperature. The percentages of α-helix, β-sheet, and coil plus turn were estimated from the measured ellipticities by using a multilinear least-squares program based on data from Greenfield and Fasman (1969). Prediction of secondary structure was achieved by running the algorithm of Garnier (1978) without introducing any decision constant for each type of 2D structure. Calculations were made with ANTHEPROT 5.5 (Deléage *et al.*, 1988).

Mass Spectroscopy. Electrospray mass spectroscopy analysis was performed on a VG Trio II electrospray mass spectrometer. The protein sample was dissolved in 50% acetonitrile and 1% formic acid. The sample was delivered to the nebulizer head by pumping 10 μL of the solution (5 μg) in 5 min.

Nucleotide Hydrolysis. The ATPase or GTPase activity of DNα19 was assayed in 100 μL of buffer G with 20 μM [γ-^{32}P]NTP (600 000 cpm/assay), at a protein concentration of 10 μM. After various time of incubation at 25 °C, the reaction was stopped by addition of 100 μL of 1 M perchloric acid. The $^{32}P_i$ produced by NTP hydrolysis was titrated according to the method of Conway and Lipmmann (1964) adapted to small volumes. For assay in the presence of ADP, DNα19 was preincubated for 5 min with ADP before the measurement of ATPase activity.

Protein Measurements. The protein content was estimated using the micro BCA protein assay reagent from Pierce. The concentration of purified DNα19 was also measured from its UV absorbance at 280 nm, using a molar extinction coefficient of 22 900 M^{-1} cm^{-1} at pH 5.0. This value was deduced from the molar extinction coefficient of DNα19 in 0.1 M NaOH, using a molar extinction coefficient of 2390 M^{-1} cm^{-1} at 294.4 nm for both tyrosine and tryptophan residues (Beaven & Holidays, 1952), taking into account that DNα19 contains eight tyrosine and two tryptophan residues.

RESULTS

Limits of the Nucleotide-Binding Domain. The limits of the putative nucleotide-binding domain (NBD) of the α subunit were chosen by comparison of the whole subunit with proteins classified in the same mononucleotide-binding chain family (Schulz, 1992) that have a resolved 3D structure: adenylate kinase (Diederichs & Schulz, 1991), guanylate kinase (Stehle & Schulz, 1990), H-*ras* p21 (Pai *et al.*, 1990), and EF-Tu (Lacour *et al.*, 1985). A preliminary alignment of the primary structures was carried out with respect to the best conserved signature sequence of these nucleotide-binding proteins, which is the P loop (Saraste *et al.*, 1990). This showed clearly two common features of the NBDs of the reference proteins, suggesting that they could also be present in the α subunit: they begin just before the P loop and contain 170–190 residues.

A further comparison of the sequences, carried out by hydrophobic cluster analysis (Gaboriaud *et al.*, 1987) and a set of predictive methods [hydropathy (Kyte & Doolittle, 1982), 2D structure (Garnier *et al.*, 1978), packaged in ANTHEPROT 5.5 (Deléage *et al.*, 1988)], revealed several additional similarities between the sequence of H-*ras* p21 and the region between the residues R_{165} and T_{330} of the α subunit. This is illustrated in Figure 1, which displays the alignment of the HCA plot, the 2D structure deduced from crystallographic data of H-*ras* p21, and the predicted 2D structure of the selected region of the α subunit. These methods revealed a similarity between the segments β_1–L_3 of both sequences, as well in the distribution of their hydrophobic clusters as in their exact or predicted 2D structure. The N-terminal region of H-*ras* p21 is known to play a critical role in the binding of the nucleotide, since 10 residues of this region interact directly with either the polyphosphate chain or the ribose moiety [circled residues in Figure 1; data from Pai *et al.*, (1990)]. Besides the P loop L_1, the comparison highlights the putative L_2 loop, in which residues W_{35} and S_{38} can be aligned to F_{28} or Y_{32} and T_{35} of H-*ras* p21. These observations, added to the assumption that the N-terminus of the NBD could be near the A motif (GX_4GKT/S; Walker *et al.*, 1982, 1985; loop L_1 in Figure 1), led us to choose the residue R_{165} as the first residue of the NBD (R_7 in the sequence of DNα19). This residue is located, like the residue K_5 of H-*ras* p21, just before the sheet β_1.

Concerning the choice of the C-terminal residue, no well-conserved signature sequence such as the P loop was found. However, comparison of the HCA plots of H-*ras* p21 and the selected region of the α subunit revealed two similar patterns shown by a dashed area in Figure 1, in a region where 4 residues of H-*ras* p21 interact with the base or the ribose moiety of the nucleotide. The latter observation suggested that this α-subunit region could also be critical for the interaction with the nucleotide, and the sequence was thus stopped after the following 2D structure at the residue T_{330}. The estimation of the hydrophilicity indicated that the selected polypeptide is mainly hydrophilic, in contrast to the other parts of the whole subunit.

Purification of DNα19. The resulting gene produced by the insertion of DNATP1 in pT7-7 encodes a recombinant protein corresponding to the fusion of the sequence MARIRA (in italic in the following sequence) given by the polylinker of pT7-7 with the region R_{165}–T_{330} of the α subunit in which Q_{167} is replaced by a serine residue (underlined in the following sequence). The complete sequence of the deduced protein is thus

```
  1 MARIRARGSR ELIIGDRQTG KTAIALDTIL NHKRWNNSSD ESKKLYCVYV
 51 AVGQKRSTVA QLVQKLEEND SLKYSIIVAA TASESAPLQY LAPFSGCAMG
101 EWFRDNGKHG LVVYDDLSKQ AVAYRQMSLL LRRPPGREAY PGDVFYLHSR
151 LLERAAKMSP KHGGGSLTAL PVIET
```

This polypeptide, called DNα19, is 175 residues long, with a molecular mass of 19 424 Da and a theoretical isoelectric point of 10.02.

The recombinant protein was produced at high levels but always in an aggregated form, whatever the duration (between 0 and 30 min) and temperature (between 37 and 42 °C) of the heat induction. The inclusion bodies were extensively washed in a buffer containing, first, 2% sodium deoxycholate and then 1% Triton X-100 and 2 M NaCl. This treatment eliminates the major part of bacterial proteins as shown in Figure 2A, lanes 2 and 3, observed by SDS–PAGE (Laemmli, 1970) and gives an inclusion-bodies fraction greatly enriched in the overexpressed polypeptide (lane 4). The proteins of lower apparent molecular weight than DNα19 were also found under the same conditions of culture without DNATP1 inserted in pT7-7 (not shown), indicating that they are not generated by a proteolytic degradation of DNα19.

The concentration of Gdn-HCl ensuring a selective solubilization of DNα19 was determined on 50-μL aliquots of washed aggregates, treated with increasing concentrations of the denaturing agent, dialyzed as previously described (Falson, 1992), and analyzed by SDS–PAGE. A concentration of 3 M Gdn-HCl was found to solubilize DNα19 completely

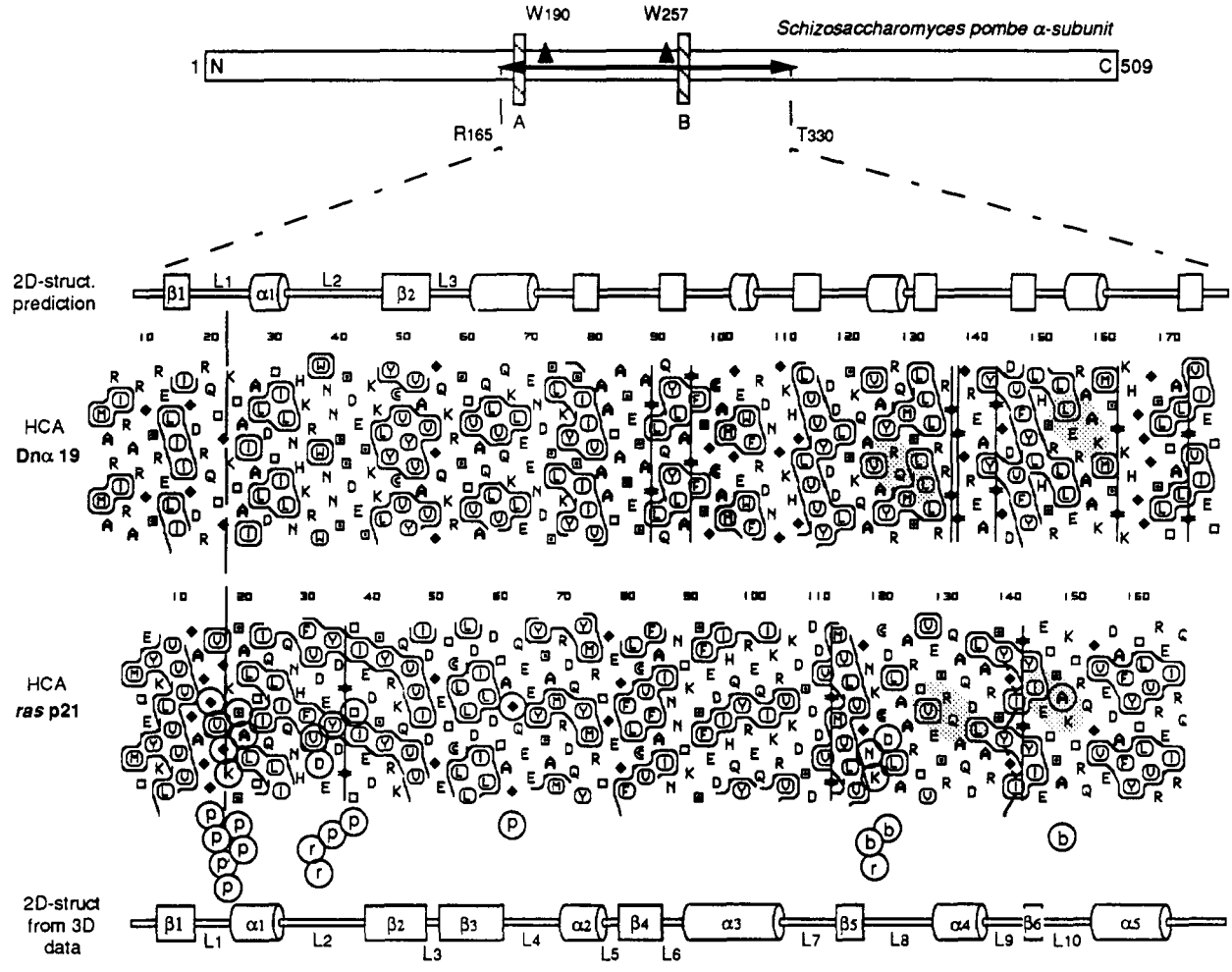

FIGURE 1: Alignment of the HCA plots of the putative nucleotide-binding domain of the α subunit with the sequence of H-*ras* p21. A schematic drawing of the whole α subunit is displayed at the top of the figure to locate DNα19, both Walker motifs A $_{170}GX_4GKT_{177}$ and B $_{259}RX_6h_4D_{270}$ (Walker *et al.*, 1982, 1985), and tryptophan residues used for the fluorescence experiments. DNα19 corresponds to the region R_{165}-T_{330} of the α subunit preceded by 6 residues added by the genetic construction, as described under Materials and Methods. R_{165} of the α subunit thus corresponds to R_7 of DNα19. Sequences of DNα19 and H-*ras* p21 are aligned on the lysine residue of the motif A, which is shown by a vertical broken line. Circled amino acids of H-*ras* p21 are those interacting directly with the GTP, as shown under the HCA plot of H-*ras* p21 at the corresponding place by a circled p, r, and b, indicating the interaction with the polyphosphate chain, the ribose, and the base moiety, respectively (Pai *et al.*, 1990). As described by Lemesle *et al.* (1990), hydrophobic residues (VLIFMYW) of the HCA plots are contoured and called hydrophobic clusters; proline, glycine, serine, and threonine residues are represented by a star, a diamond, a square, and a square with a point, respectively. Dashed areas show particular similarity between both sequences. The secondary structure, either predicted for DNα19 (Garnier *et al.*, 1978; no decision constant) or deduced from crystallographic data for H-*ras* p21 (Pai *et al.*, 1990), is indicated; α-helix, β-sheet, and loop are represented by a cylinder, a box, and a line, respectively.

(Figure 2A, lane 5), while the set of proteins migrating in SDS–PAGE around 31 kDa remained insoluble (Figure 2A, lane 4). This was particularly helpful for the following chromatographic step since, with the exception of these contaminating proteins, DNα19 was the first protein eluted from the reversed-phase column, as shown in Figure 2B (peak 1). The electrophoresis analysis of the elution pattern shows that DNα19 was pure after the reversed-phase chromatography. However, this chromatographic step was carried out again on the first pool to increase the purity of the fraction (Figure 2A, lane 6). The first 20 residues of the recombinant DNα19 were sequenced (not shown), revealing the processing of the N-terminal methionine, in agreement with the N-end rule in *E. coli*. Electrospray mass spectroscopy analysis of the purified polypeptide (not shown) indicated the good homogeneity of the preparation. The average of the mass values obtained for the differently charged peaks gave a mean value of 19 299 ± 5 Da, which corresponds well to the deduced molecular mass value of 19 294 Da for the recombinant protein lacking the N-terminal methionine residue.

Refolding of DNα19. The polypeptide was refolded by using the high-dilution technique described by Jaenicke and Rudolph (1990) to lower the probability of intermolecular interactions. The refolding of the polypeptide was followed by optical absorbance to detect the formation of aggregates (not shown) and evaluated by circular dichroism and intrinsic fluorescence, as shown in Figure 3. The protein stored in 0.1% TFA was first lyophilized and then solubilized in water at high concentration. In this form, DNα19 did not precipitate with time but was virtually devoid of 3D structure as checked by CD (not shown here, the corresponding CD spectrum looked like curve 3 of Figure 3A) or by ^{1}H NMR (F. Penin, unpublished results). The concentrated protein was then highly and rapidly diluted, the temperature being maintained at 25 °C. The best solubility and stability, *i.e.*, conditions ensuring that no protein precipitation occurred either immediately or with time, were found with an organic buffer: 25 mM Mes buffered at pH 5.0 with Tris, having a low ionic strength, 25 mM NaCl, containing 1 mM 2-mercaptoethanol, and 1 mM $MgCl_2$. We found that the protein sample had to be incubated for at least 8 h at 25 °C before a stable intrinsic fluorescence emission spectrum could be obtained, indicating that complete folding occurs at a low rate. After this period, the fluorescence emission spectrum did not change, even for

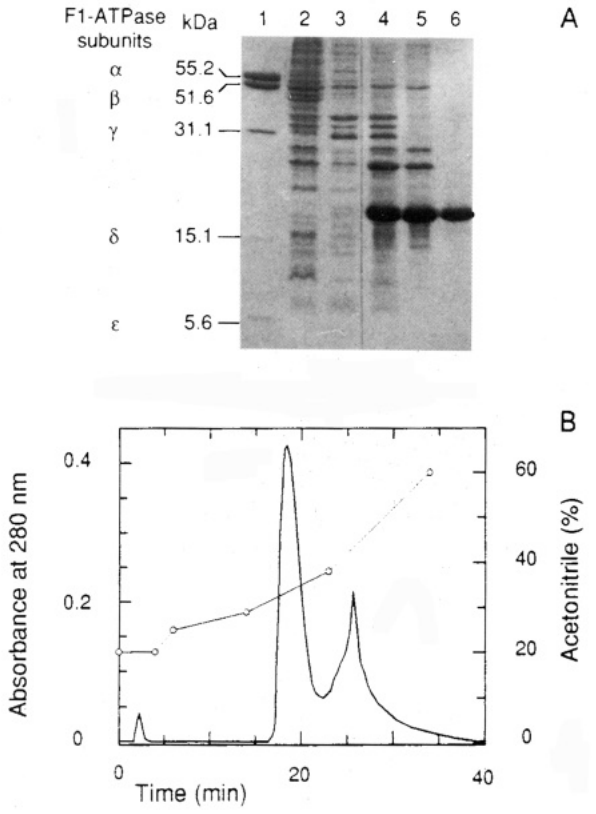

FIGURE 2: Purification of DNα19. (A) SDS–PAGE of the intermediate fractions of DNα19. (Lane 1) Pig heart F_1-ATPase subunits used here as molecular weight markers with the corresponding values indicated on the left edge (5 μg); (lanes 2 and 3) supernatant fractions of the first and second washing steps, respectively; (lane 4) washed pellet of inclusion bodies; (lane 5) supernatant fraction after solubilization of the inclusion bodies by 3 M guanidine hydrochloride; (lane 6) eluate fraction of the reversed-phase chromatography step (15 μg). The electrophoresis was performed as described by Laemmli (1970) on a 16% acrylamide gel. (B) Elution profile of the reversed-phase chromatography. One milligram of protein in 0.1% TFA was submitted to the reversed-phase chromatography as described under Materials and Methods. The gradient of acetonitrile in 0.1% TFA is indicated with open circles. The main peak corresponds to DNα19.

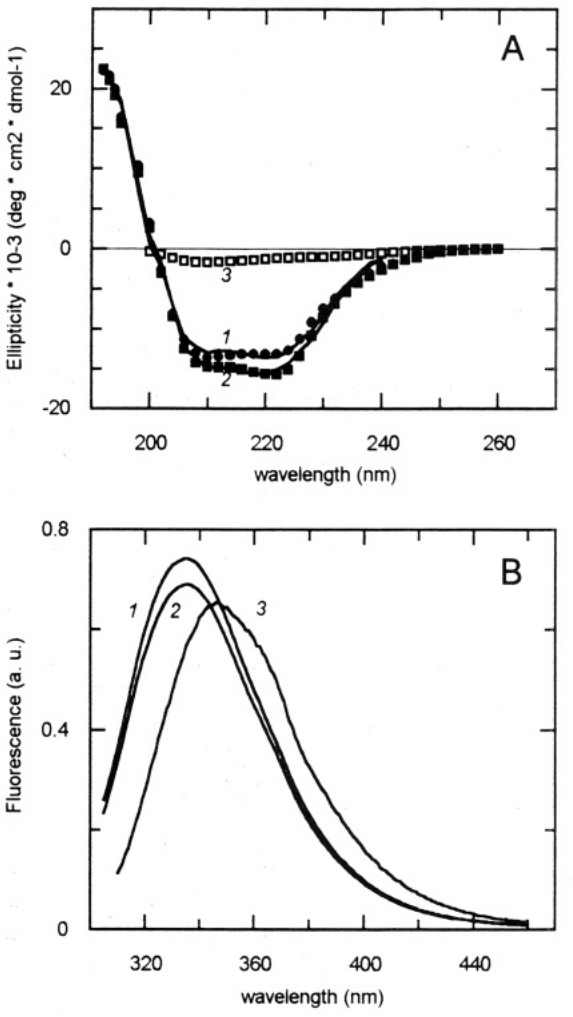

FIGURE 3: Circular dichroism and intrinsic fluorescence analysis of folded and unfolded DNα19. DNα19 was diluted at 2 μM either in the buffer G, in the absence (1, solid circles) or the presence (2, solid squares) of a stoichiometric amount of ATP, or in buffer G containing 6 M Gdn-HCl (3, open squares). After an 8-h incubation at 25 °C, each solution was submitted to circular dichroism and intrinsic fluorescence emission analysis as shown in panels A and B, respectively. Spectra were recorded as described under Materials and Methods.

an incubation time as long as 72 h. Under these conditions, DNα19 displayed a CD spectrum (Figure 3A, curve 1) and an intrinsic fluorescence emission spectrum (Figure 3B, curve 1) typical of a folded protein, as compared to the respective spectra produced by DNα19 in solution in 6 M Gdn-HCl (Figure 3, curves 3). The CD spectrum of the folded protein displays bands over 200 nm consistent with a mixed α and β structure. The fitting of the CD data carried out as described under Materials and Methods indicated that DNα19 is constituted of 32.7 ± 1.3% α-helix, 19.2 ± 4.2% of β-sheet, and 20.8 ± 2.4% coil plus turn (sum = 73%). The maximal intrinsic fluorescence emission of the folded protein was found at 335 nm (Figure 3B, curve 1). Denaturation in 6 M Gdn-HCl led to a red shift of 12 nm and a quenching of 12% (Figure 3B, curve 3 compared to curve 1).

The presence of a stoichiometric amount of ATP during the equilibration step accelerated the folding approximately 2 times (not shown). A limited modification of the CD spectrum of the protein folded in the presence of ATP (Figure 3A, curve 2) is observed when compared to the CD spectrum produced by the same protein folded in the absence of nucleotide (Figure 3A, curve 1). This suggests that DNα19 is more folded in the presence of nucleotide. Notably, the percentages of secondary structures estimated in that case [33.2 ± 1.4% α-helix, 34.2 ± 2.6% β-sheet, and 34.3 ± 2.6% of coil plus turn (sum = 103%)] by fitting of the CD data of DNα19 folded in the presence of ATP are close to those obtained by 2D structure prediction, 31, 32, and 37%, respectively. The presence of nucleotide during the folding step induces a similar limited effect on fluorescence emission spectrum with a quenching of 7% and neither red nor blue shift (Figure 3B, curve 2) as compared to the protein sample without nucleotide (curve 1).

Nucleotide Binding to DNα19 Monitored by Fluorescence Experiments. The incubation of DNα19 with increasing concentrations of adenine or guanine nucleotides led to a progressive intrinsic fluorescence quenching without any shift of the emission spectrum, giving the monophasic saturation curves displayed in Figure 4A,B. A maximal effect was obtained for a nucleotide concentration around 30 μM. It is worth mentioning that DNα19 precipitated at ATP or GTP concentrations higher than 50 μM, while it remained fully soluble in the presence of millimolar concentrations of ADP and GDP. GTP and GDP induced 27 and 18% quenchings, higher than those obtained with ATP and ADP (21 and 17%, respectively; Table I). Noteably, a 4–9% higher quenching was produced by triphosphate than by diphosphate nucleotides. The fitting of each saturation curve, carried out as described under Materials and Methods, was consistent with the binding

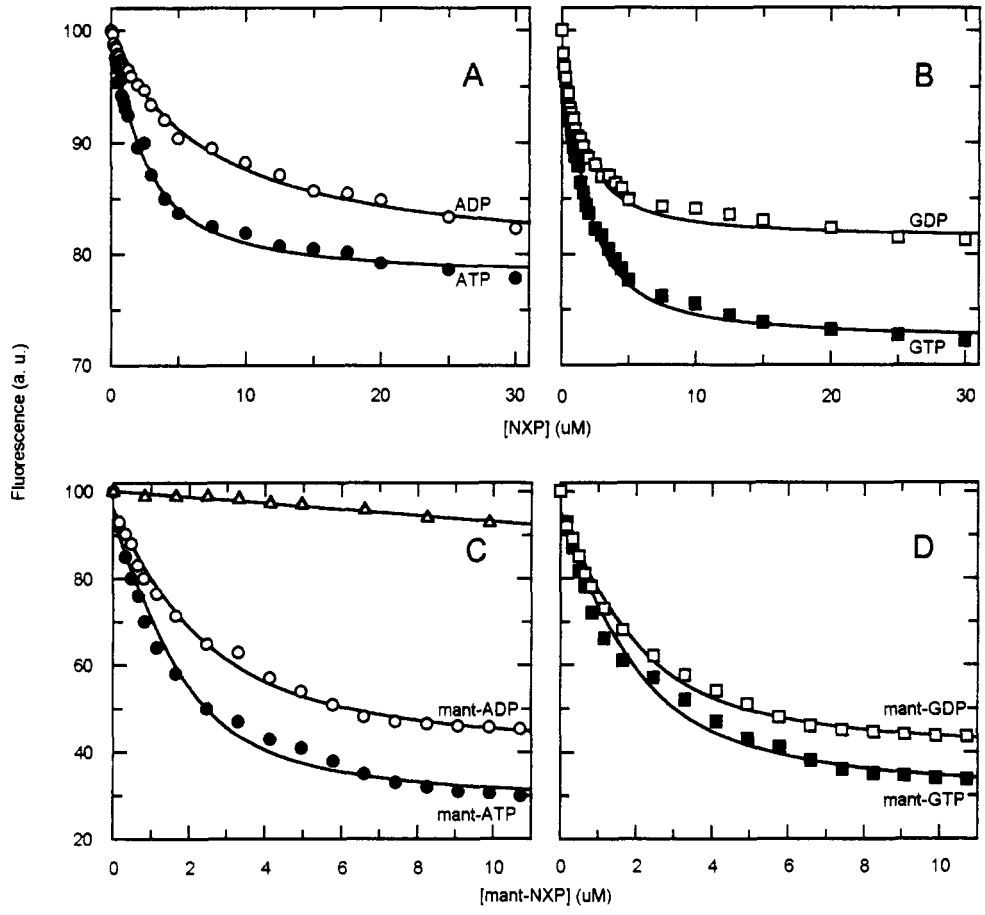

FIGURE 4: Binding of nucleotides and analogues to DNα19 as monitored by the quenching of intrinsic fluorescence. The preparation of the protein sample (DNα19 equilibrated in the buffer G at 2 μM) and the recording of the fluorescence spectra are detailed under Materials and Methods. Increasing nucleotide concentrations were added, and after 5 min of incubation, the spectra were collected between 310 and 380 nm upon excitation at 295 nm. Data are indicated in percent of the emission spectrum area recorded before the nucleotide addition (a typical spectrum is displayed in Figure 5B, curve 1). All the curves were fitted by using eq1 described under Materials and Methods. Panels A, B, C, and D display the curves of fluorescence quenching obtained by incubating DNα19 with ADP and ATP, GDP and GTP, Mant-ADP and Mant-ATP, and Mant-GDP and Mant-GTP, respectively. Di- and triphosphate nucleotides are indicated with open and solid symbols, respectively. Panel C also shows in addition the residual quenching of intrinsic fluorescence obtained with Mant-ADP when DNα19 was first denatured for 2 h with 6 M Gdn-HCl (open triangles).

Table I: Binding Parameters of Nucleotides and Derivatives Deduced from Fluorescence Experiments[a]

nucleotide or analogue	intr fluo		extr fluo	FRET
	ΔF (%)	K_d (μM)	K_d (μM)	K_d (μM)
ATP	21	2.14 (±0.16)		
ADP	17	5.38 (±0.51)		
GTP	27	1.70 (±0.09)		
GDP	18	2.31 (±0.13)		
Mant-ATP	69	0.59 (±0.15)	0.28 (±0.17)	0.20 (±0.07)
Mant-ADP	57	1.17 (±0.21)	0.55 (±0.18)	0.50 (±0.11)
Mant-GTP	69	0.80 (±0.22)	0.18 (±0.11)	0.24 (±0.07)
Mant-GDP	56	0.80 (±0.15)	0.16 (±0.10)	0.41 (±0.14)

[a] The maximal quenching of intrinsic fluorescence ($\Delta F = F_{Ci} - F_{Cf}$) of DN$\alpha$19, in the presence of a saturating concentration of nucleotides or Mant derivatives, and the corresponding dissociation constant, K_d, were determined from data of Figures 4 and 5. The fitting of F_{Ci}, F_{Cf}, and K_d was achieved as described under Materials and Methods, by introducing eq 1 in Grafit; the enzyme concentration was fixed at 2 μM. Standard deviations are indicated in parentheses.

of one nucleotide per DNα19. The dissociation constant values of the protein–nucleotide complex were found to be lower for the guanine nucleotides (1.70 and 2.31 μM for GTP and GDP, respectively) than for the adenine ones (2.14 and 5.38 μM for ATP and ADP, respectively), the affinity of DNα19 being better for the triphosphate species.

As shown in Figure 4C,D, the incubation of DNα19 with the Mant derivatives of nucleotides led to a maximal quenching of intrinsic fluorescence of 56–69% (Table I). This quenching value was reached with analogue concentrations lower than 10 μM. As for the unmodified nucleotides, the triphosphate analogues produced a higher quenching than the diphosphate ones. The specificity of the analogue binding was checked both by competition experiments (see below) and by monitoring Mant-ADP binding to DNα19 in the presence of 6 M Gdn-HCl. Under the latter condition, only residual quenching of the intrinsic fluorescence was observed (Figure 4C, triangles). The curve fitting was consistent with the binding of one analogue per polypeptide. The deduced K_d values ranged between 0.59 and 1.17 μM depending on the nucleotide studied (Table I). Noteworthy, these K_d values are significantly lower than those of the corresponding unmodified nucleotides.

The binding of the Mant derivatives was also measured by the enhancement of the extrinsic fluorescence emission of the methylanthraniloyl group. As shown in Figure 5A,B, the fluorescence of the Mant group was enhanced 2-fold upon binding of the nucleotide derivative to the polypeptide, at a concentration lower than 8 μM. The specificity of fluorescence enhancement was checked with ADP by competition with the bound Mant-ADP (inset of Figure 5A). ADP was found to reverse efficiently the enhancement with a half-maximal effect at 30 μM. The calculated dissociation constant values of each Mant derivative–protein complex (Table I) were 2–4-fold lower than those obtained with the intrinsic fluorescence experiments. Preliminary studies of stopped-flow experiments

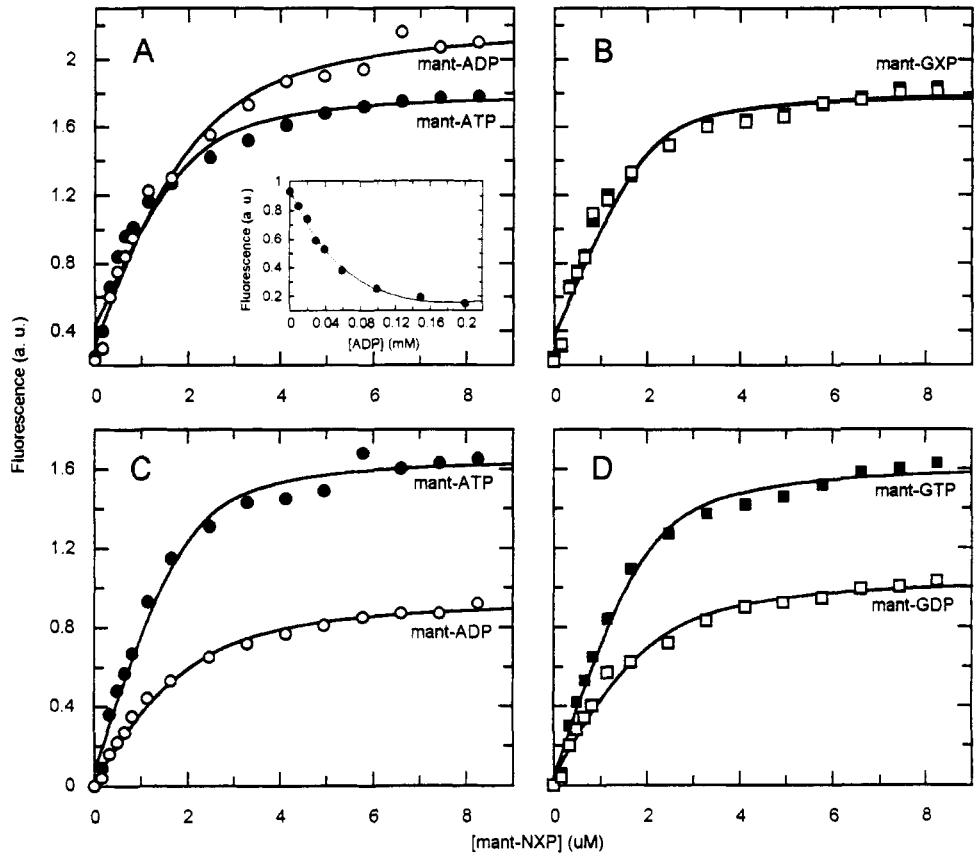

FIGURE 5: Binding of Mant derivatives monitored by extrinsic fluorescence and resonance energy transfer. Experimental conditions and symbols used for each type of nucleotide are the same as those of Figure 4. All the curves were fitted by using the eq 1 described under Materials and Methods. (A and B) Extrinsic fluorescence enhancement of the methylanthraniloyl group of Mant-nucleotides was recorded at 450 nm, upon excitation at 350 nm, as a function of the concentration of adenine or guanine Mant-nucleoside di- or triphosphates. (Inset of panel A) Chase of bound Mant-ADP, added at a 1 μM concentration, by increasing concentrations of ADP and followed under the conditions of extrinsic fluorescence emission assay. (C and D) Enhancement of the fluorescence resonance energy transfer between indole and methylanthraniloyl groups as a function of the concentration of Mant derivatives of adenine or guanine nucleoside di- or triphosphates. The wavelengths of excitation and emission were 295 and 450 nm, respectively.

indicated that the half-time for binding, at a concentration of 10 μM Mant derivative, was lower than 1 ms (G. Divita, unpublished data).

A resonance energy transfer between the tryptophan residues of DNα19 and the Mant group of the nucleotide analogues was observed when the excitation wavelength was fixed at 295 nm (Figure 5C,D). The efficiency of energy transfer was dependent on the Mant derivative concentration, and as for the intrinsic or extrinsic fluorescence experiments, the maximal effect was obtained at a concentration lower than 8 μM. The estimated dissociation constants (Table I) were in the same range as those obtained by extrinsic fluorescence.

The existence of FRET between the indole and Mant groups allows the estimation of the distance between the two groups. This was carried out as described under Materials and Methods, using eqs 2–7, and the results are listed in the Table II. The transfer efficiency was estimated by two methods, considering either the decrease in the donor fluorescence (E_1) or the increase in the acceptor fluorescence (E_2). As shown in Table II, E_2 was always higher than E_1. However, the deduced distances, R_1 and R_2, between the indole group and the Mant moiety, calculated by both methods, are quite similar, the difference being in the range of 0.5–0.7 Å. They are always 1.5–2.5 Å lower for the triphosphate than for the diphosphate nucleotides: 11.5–11.0 and 11.8–11.2 Å for Mant-ATP and Mant-GTP, respectively, as compared to 14.0–13.3 and 13.5–12.9 Å for Mant-ADP and Mant-GDP, respectively.

Hydrolytic Activity of DNα19. As shown in Figure 6, the incubation of DNα19 with a 2-fold molar excess of [γ-^{32}P]ATP

Table II: Estimated Parameters from the FRET Experiments and Deduced Distances between Indole and the Mant Group of Each Derivative[a]

	efficiency				R^b	
acceptor	E_1 (%)	E_2 (%)	overlap J	R_0 (Å)	R_1 (Å)	R_2 (Å)
Mant-ATP	76	80	6.1×10^{-16}	14	11.5	11.0
Mant-ADP	50	58	6.1×10^{-16}	14	14.0	13.3
Mant-GTP	74	79	5.9×10^{-16}	14	11.8	11.2
Mant-GDP	52	61	5.9×10^{-16}	14	13.5	12.9

[a] The parameters used for the distance calculations were deduced from the data of FRET displayed in Figure 5C,D and using eqs 2–7 described under Materials and Methods. [b] The distances R_1 and R_2 were calculated by using in eq 4 the transfer efficiency estimated with methods 1 and 2. The error in the distance estimation is less than 10%.

or GTP produced with time a low but significant amount of inorganic phosphate, indicating that hydrolysis occurred. In these conditions, the hydrolytic rates of ATP and GTP were 0.0047 and 0.0033 min^{-1}, respectively. The same hydrolytic rates were obtained whatever the concentrations of DNα19 (2–10 μM) and nucleotides (10–50 μM) tested. The specificity of the reaction was checked in two ways: (i) the presence of excess ADP induced a complete inhibition of the hydrolysis (lower curve with open circles in Figure 6); (ii) no $^{32}P_i$ due to a contaminating phosphatase activity was detected after incubation of DNα19 with a 4-fold excess of [α-^{32}P]ATP, even for a time as long as 120 min (not shown). In addition, the experiment was carried out with two independently purified pools of the protein, refolded with or without ATP to exclude the presence of a contaminating kinase or ATPase. The same

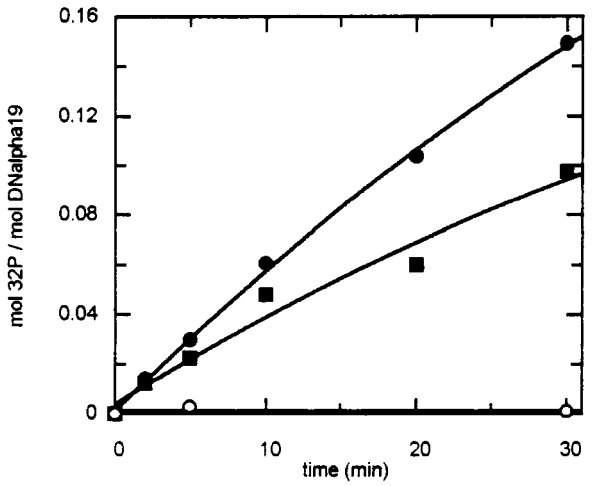

FIGURE 6: Hydrolysis of [γ-^{32}P]NTP by DNα19. Assay conditions were as described under Materials and Methods. One nanomole of protein was incubated in 100 μL of buffer G (final protein concentration 10 μM) at 25 °C in the presence of 2 nmol of either labeled GTP (solid squares) or labeled ATP, with (open circles) or without (solid circles) 50 μM ADP. The reaction was stopped by the addition of perchloric acid. The $^{32}P_i$ produced was then extracted and counted. Each value was corrected for the quantity of $^{32}P_i$ produced without protein in the same time of incubation (blank).

rates of hydrolysis were obtained with the two protein samples.

DISCUSSION

The results presented here demonstrate that the α subunit of the yeast F_1-ATPase contains a nucleotide-binding domain that can be obtained as a soluble form. It is able to interact with either adenine or guanine nucleotides and is also able to hydrolyze ATP and GTP.

Design and Production of DNα19. Since the whole α subunit of the yeast enzyme could not be isolated from the other subunits in a soluble form without using high concentrations of denaturing agents such as 6 M Gdn-HCl or 8 M urea (P. Falson, unpublished data), it was impossible to use an experimental strategy involving a mild proteolysis of the isolated subunit followed by the identification of a fragment able to bind a nucleotide. Therefore, we conceived the DNα19 domain by comparison of the α-subunit sequence with those of other nucleotide-binding proteins and produced it by genetic engineering.

The large number of publications dealing with the comparison between nucleotide-binding proteins (Walker *et al.*, 1982; Fry *et al.*, 1986; Saraste *et al.*, 1990; Schulz, 1992, and references cited therein) allowed the comparison of the α subunit with only a limited number of proteins having a related mononucleotide-binding chain fold. Hydrophobic cluster analysis has proven to be very efficient (Lemesle *et al.*, 1990) to compare protein sequences on the basis of the distribution of the hydrophilic and hydrophobic residues (Gaboriaud *et al.*, 1987). The use of HCA together with a prediction method highlights the similarity between the segments β_1–L_3 from DNα19 and H-*ras* p21, suggesting for the first time that the predicted loop L_2 of DNα19 might be functionally equivalent to that of H-*ras* p21 and therefore might play a critical role in nucleotide binding. The choice of the region R_{165}–T_{330} of α subunit as a putative nucleotide-binding domain is in good agreement with the proposal of Maggio *et al.* (1987), suggesting that the region spanning residues 160–340 of the *E. coli* enzyme α subunit could constitute the nucleotide-binding domain.

The polypeptide was produced as a nonsoluble material whatever the conditions of induction time and culture temperature tested and reported elsewhere to influence the formation of aggregates (Schein, 1989). In counterpart, the overexpression as inclusion bodies and the small size of DNα19 allowed a rapid purification of an unfolded form of the polypeptide using an efficient washing step of the inclusion bodies, a specific solubilization of the polypeptide, and a reversed-phase chromatography. SDS–PAGE and mass spectrometry analyses showed that a high degree of purity was reached. This strategy can be applied to any protein produced as inclusion bodies.

The refolding process of DNα19 can be disected into solubilization and equilibration steps. The solubilization was carried out without loss of material by a high-dilution step. Ionic strength and pH of the buffer used during and after the dilution step were found to be critical parameters for the long-term solubility of the polypeptide. In contrast to the solubilization, the equilibration of the protein is very slow. Evidence that the polypeptide reaches a folded and stable state was provided by the spectroscopic methods used, CD and intrinsic fluorescence. The latter indicated that the tryptophan residues are in a nonpolar environment, as also observed for most proteins in the native state (Etfink, 1991). Conclusive observation that, when refolded, DNα19 adopts a native-like conformation comes from its capacity to hydrolyze ATP and, more slowly, GTP. The low rate of ATP hydrolysis, 0.0047 min^{-1}, is comparable to the value found for H-*ras* p21 (0.02 min^{-1} with GTP and 0.005 min^{-1} with GTPαS; Tucker *et al.*, 1986). Although the meaning of this low hydrolytic activity remains unclear, its finding was not surprising since DNα19 contains the sequence GX_4GKT, in which the lysine residue is thought to play a critical role in the mechanism of hydrolysis (Saraste *et al.*, 1990).

Nucleotide Binding to DNα19. DNα19 contains the two tryptophan residues, W_{35} and W_{102}, of the α subunit (corresponding to W_{190} and W_{257} in the whole subunit), strategically positioned with respect to the Walker A and B motifs (Falson *et al.*, 1991) and reported to constitute a powerful probe for nucleotide binding to the yeast enzyme (Divita *et al.*, 1991, 1992). The present intrinsic fluorescence experiments provide evidence that the domain binds adenine or guanine nucleotides with a 1:1 stoichiometry and a K_d ranging from 1.7 to 5.4 μM. Extrapolation of these results to the entire subunit would indicate a difference with the *E. coli* α subunit, since the latter protein was shown to be specific for adenine nucleotides (Perlin *et al.*, 1984). On the other hand, DNα19 displays the same type of differential affinity for ATP and ADP as reported for the *E. coli* α subunit (0.1 and 0.9 μM, respectively: Dunn & Futai, 1980). This suggests that the selectivity for adenine nucleotides of the α-subunit binding domain inside native F_1-ATPase might be essentially due to interaction with the β subunit. This is consistent with affinity labeling experiments of noncatalytic sites suggesting an interaction of the nucleotide base moiety with the β subunit (Cross *et al.*, 1987; Bullough *et al.*, 1988). In addition, the Mant derivatives give the same type of results as unmodified nucleotides, although the quenching is much higher. This suggests that one tryptophan residue at least is located nearer the Mant group than the base of the nucleotide.

The study of nucleotide binding by extrinsic fluorescence experiments confirms that DNα19 is able to bind 1 mol of nucleotide analogue/mol. The binding of the Mant derivatives of adenine and guanine nucleotides induces a 2-fold enhancement of the fluorescence emission, indicating that the nucleotide-binding site has a low polarity as proposed for other analogues (Dupont & Pougeois, 1983). Similar enhancement values were obtained when the same nucleotides bound to the

```
                -pα1-> <------pL2-----> <--pβ2--
[1]  180 ATDTIL NQK.........GQG VICVYVAI 199   chloroplast
[2]  179 AIDTIL NQK.........GED VICVYVAI 198   cyanobacterium
[3]  179 AIDTII NQK.........DQN MICIYVAI 198   thermophilic bacterium
[4]  179 AIDAII NQR.........DSG IKCIYVAI 198   enterobacterium
[5]  179 ALDTIL NQKVYNDAAGDDESKK LYCVYVAI 208  photosynthetic bacterium
[6]  181 AIDTIL NQKQLNS.RATSESET LYCVYVAI 209  plant mitochondrion
[7]  179 AIDTII NQKRFND..GTDEKKK LYCIYVAI 206  mammalian mitochondrion
[8]  180 ALDTIL NHKRWNN..SSDESKK LYCVYVAV 207  yeast mitochondrion

     020 TIQLIQ NHFVDEYD.PTI EDSYRKQVVIDG 048  H-ras p21
         --α1-> <----L2----> <---β2--->
```

FIGURE 7: Comparison of the putative loop L_2 of the α subunit from various organisms to the loop L_2 of H-*ras* p21. The partial sequences of the α subunits indicated here were chosen to give a representative panel of organelles and organisms: [1] *chloroplast* (wheat, Howe *et al.*, 1985); *bacteria* [2] cyanobacterium (*Synechococcus* 6301, Cozens & Walker, 1987), [3] thermophilic bacterium (PS3; Ohta *et al.*, 1988), [4] enterobacterium (*E. coli*, Walker *et al.*, 1985), [5] photosynthetic non-sulfur bacterium (*R. blastica*; Tybulewicz *et al.*, 1984); *mitochondria* [6] plant (*Nicotiana plumbaginifolia;* Chaumont *et al.* 1988), [7] yeast (*S. pombe*; Falson *et al.*, 1991), [8] mammalian (bovine heart; Walker *et al.*, 1985). The segment of each α-subunit sequence is numbered both at left and right edges. Predicted secondary structures of the segment of each α subunit are indicated by $p\alpha_1$, pL_2, and $p\beta 2$ for *putative* α-helix 1, loop 2, and β-sheet 2, respectively. The exact secondary structure of the segment 20–48 of the H-*ras* p21 sequence is from Valencia *et al.* (1991). The gaps indicated by a point have been introduced with respect to the longest sequence of the α subunit.

whole F_1-ATPase from *S. pombe* (Divita *et al.*, 1993b) or to H-*ras* p21 (John *et al.*, 1990). In addition, the analogue binds to the same site similarly as the unmodified nucleotide since Mant-ADP is completely displaced by excess ADP. The affinity was found to be 5 times higher than for the corresponding nucleotides; a similar effect is seen with myosin, where Mant-ADP binds more strongly than ADP (Woodward *et al.*, 1991). The K_d values for the binding of Mant-ATP (0.28 μM) and Mant-ADP (0.55 μM) are much lower than those reported for the interaction between the recombinant rat liver α subunit and trinitrophenyl-ATP (TNP-ATP, 1–5 μM) or TNP-ADP (10–50 μM) (Lee *et al.*, 1989). These differences do not seem to be only due to the type of analogue used, since K_ds lower than the micromolar range were also obtained when using TNP-ATP or TNP-ADP with DNα19 (P. Falson, unpublished results).

The large spectral overlap that exists between the fluorescence emission of the tryptophan indole group and the absorption of the Mant group of the nucleotide analogue leads to the expectation that fluorescence resonance energy transfer between these groups might occur; this is indeed the case. It was found to be more pronounced for the triphosphate than for the diphosphate nucleotides, as also observed for intrinsic fluorescence quenching. Calculation of the distance between both groups by using a set of Mant derivatives shows a significant difference depending on the length of the phosphoanhydride chain of the nucleotide analogue. This result suggests that a tryptophan residue is located within the binding site of the domain, near the polyphosphate side of the nucleotide, in tight interaction with the aromatic ring of the Mant group. The recent finding that αW_{190} of native yeast F_1-ATPase (W_{35} in DNα19) tightly interacts with ADP bound to the α-subunit noncatalytic site (Divita *et al.*, 1993a) strongly suggests that W_{35} is the residue involved in the process of energy transfer. This observation strengthens the idea proposed above that the putative L_2 loop containing W_{35} plays a critical role in nucleotide binding.

Functional Role of the Nucleotide-Binding Domain of the α Subunit. DNα19 constitutes the major part of the α-subunit contribution to the noncatalytic site in the yeast F_1-ATPase [see, for reviews, Penefsky and Cross (1991) and Allison *et al.*, (1992)]. The complete domain would be slightly longer on the C-terminal side according to the recent results of Weber *et al.* (1993). Previous experiments carried out with the yeast (Falson *et al.*, 1987, 1991; Jault *et al.*, 1991) and more recently with the beef heart (Jault & Allison, 1993) mitochondrial F_1-ATPases have shown that the binding of nucleotides to the noncatalytic sites is responsible for the apparent negative cooperativity, drawing the possibility that noncatalytic sites are involved in the control of catalysis. It will be of interest to know if both original features of DNα19 pointed out in this work, *i.e.*, the capacity to hydrolyze slowly triphosphate nucleosides and the putative L_2 loop probably involved in nucleotide binding, play a role in this control. In contrast, experiments carried out with the *E. coli* F_1-ATPase led Wise and Senior (1985) to the opposed conclusion, *i.e.*, that noncatalytic sites do not have any regulatory function. The putative L_2 loop could be one of the keys to explain these different behaviors since, as shown in Figure 7, the α subunits from various origins clearly display together a single marked variation of structure located precisely in this loop; depending on the origin of the protein, 1–10 residues are missing in that segment, and except for *Rhodopseudomonas blastica*, the longest putative loops are found in the mitochondrial subunit, whereas the shortest ones are found in the bacterial and chloroplast subunits. It thus appears that the putative L_2 loop could be an interesting target for insertion–deletion experiments by site-directed mutagenesis in the bacterial or yeast enzyme. Works are also in progress to characterize the kinetics properties of DNα19 and to obtain its 3D structure.

ACKNOWLEDGMENT

We thank Jean-Pierre Le Caer and Jean Rossier from the Institut Alfred Fessard (CNRS, Gif sur Yvette, France), who have carried out the mass spectroscopy experiments; Serge Leterme and André Goffeau from the Unité de Biochimie Physiologique (Louvain-La-Neuve, Belgium) for the N-terminal sequence determination; Gilbert Deléage from the Institut de Biologie et Chimie des Protéines (CNRS, Lyon, France) for the use of ANTHEPROT 5.5; and Alfred Wittinghofer from the Max-Plank Institut für Medizinische Forshung (Heidelberg, Germany) and Pierre Plateau from the Laboratoire de Biochimie de l'Ecole Polytechnique (Palaiseau, France) for critical discussion.

REFERENCES

Allison, W. S., Jault, J-M., Zhuo, S., & Pike, S. R. (1992) *J. Bioenerg. Biomembr. 24*, 469–477.

Beaven, G. H., & Holiday, E. R. (1952) *Adv. Protein Chem. 7*, 319–386.

Bullough, D. N., Brown, E. L., Saario, J. D., & Allison, W. S. (1988) *J. Biol. Chem. 263*, 14053–14060.

Chaumont, F., Boutry, M., Briquet, M., & Vassarotti, A. (1988) *Nucleic Acids Res. 16*, 6247.

Chen, R. F. (1967) *Fluorescence: Theory, Instrumentation and Practice* (Guilbault, G. C., Ed.) Dekker, New York.
Conway, T. W., & Lipmmann, F. (1964) *Proc. Natl. Acad. Sci. U.S.A. 52*, 1462–1469.
Cozens, A. L., & Walker, J. E. (1987) *J. Mol. Biol. 194*, 359–383.
Cross, R. L., Cunningham, D., Miller, C. G., Xue, Z., Zhou, J-M., & Boyer, P. D. (1987) *Proc. Natl. Acad. Sci. U.S.A. 84*, 5715–5719.
Deléage, G., Clerc, F-F., Roux, B., & Gautheron, D. C. (1988) *CABIOS 4*, 351–356.
Diederichs, K., & Schulz, G. E. (1991) *J. Mol. Biol. 217*, 541–549.
Di Pietro, A., Penin, F., Julliard, J. H., Godinot, C., & Gautheron, D. C. (1988) *Biochem. Biophys. Res. Commun. 152*, 1319–1325.
Divita, G., Di Pietro, A., Deléage, G., Roux, B., & Gautheron, D. C. (1991) *Biochemistry 30*, 3256–3262.
Divita, G., Di Pietro, A., Roux, B., & Gautheron, D. C. (1992) *Biochemistry 31*, 5791–5798.
Divita, G., Jault, J-M., Gautheron, D. C., & Di Pietro, A. (1993a) *Biochemistry 32*, 1017–1024.
Divita, G., Goody, R. S., Gautheron, D. C., & Di Pietro, A. (1993b) *J. Biol. Chem. 268*, 13178–13186.
Duncan, T. M., & Cross, R. L. (1992) *J. Bioenerg. Biomembr. 24*, 453–461.
Dunn, S. D., & Futai, M. (1980) *J. Biol. Chem. 255*, 113–118.
Dupont, Y., & Pougeois, R. (1983) *FEBS Lett. 156*, 93–98.
Etfink, M. R. (1991) *Methods Biochem. Anal. 35*, 127–205.
Fairclough, R. H., & Cantor, C. R. (1978) *Methods Enzymol. 48*, 347–379.
Falson, P. (1992) *BioTechniques 13*, 3–4.
Falson, P., Di Pietro, A., & Gautheron, D. C. (1986) *J. Biol. Chem. 261*, 7151–7159.
Falson, P., Di Pietro, A., Darbouret, D., Jault, J-M., Gautheron, D. C., Boutry, M., & Goffeau, A. (1987) *Biochem. Biophys. Res. Commun. 148*, 1182–1188.
Falson, P., Maffey, L., Conrath, K., & Boutry, M. (1991) *J. Biol. Chem. 266*, 287–293.
Förster, Th. (1948) *Ann. Phys. 2*, 55–75.
Fry, D. C., Kuby, S. A., & Mildvan, A. S. (1986) *Proc. Natl. Acad. Sci. U.S.A.. 83*, 907–911.
Futai, M., Noumi, T., & Maeda, M. (1989) *Annu. Rev. Biochem. 58*, 111–136.
Gaboriaud, C., Bissery, V., Benchetrit, T., & Mornon, J-P. (1987) *FEBS Lett. 224*, 149–155.
Gagliardi, D., Penin, F., & Gautheron, D. C. (1991) *Biochim. Biophys. Acta 1059*, 323–331.
Garnier, J., Osguthorpe, O. J., & Robson, B. (1978) *J. Mol. Biol. 120*, 97–120.
Greenfield, N., & Fasman, G. D. (1969) *Biochemistry 8*, 4108–4116.
Gromet-Elhanan, Z. (1992) *J. Bioenerg. Biomembr. 24*, 447–452.
Guerrero, K. J., Heller, L. L., & Boyer, P. D. (1990) *FEBS Lett. 270*, 187–190.
Howe, C. J., Fearnley, I. M., Walker, J. E., Dyer, T. A., & Gray, J. C. (1985) *Plant Mol. Biol. 4*, 333–345.
Jaenicke, R., & Rudolph, R. (1990) In *Protein structure, a practical approach* (Creighton, E., Ed.) pp 190–224, Practical Approach Series (Rickwood, D., & Hames, B. D., Eds.) IRL Press, Oxford, U.K.
Jault, J-M., & Allison, W. S. (1993) *J. Biol. Chem. 268*, 1558–1566.
Jault, J-M., Di Pietro, A., Falson, P., & Gautheron, D. C. (1991) *J. Biol. Chem. 266*, 8073–8078.
John, J., Sohmen, R., Feuerstein, J., Linke, R., Wittinghofer, A., & Goody, R. S. (1990) *Biochemistry 29*, 6058–6065.
Kyte, J., & Doolittle, R. F. (1982) *J. Mol. Biol. 157*, 105–132.
Lackowicz, J. R. (1983). In *Principles of fluorescence spectroscopy*, Plenum Press, New York.
Lacour, T. F. M., Nyborg, J., Thirup, S., & Clark, B. F. C. (1985) *EMBO J. 4*, 2385–2388.
Laemmli, U. K. (1970) *Nature (London) 227*, 680–685.
Lee, J. H., Garboczi, D. N., Thomas, P. J., & Pedersen, P. L. (1990) *J. Biol. Chem. 265*, 4664–4669.
Lemesle-Varloot, L., Henrissat, B., Gaboriaud, C., Bissery, V., Morgat, A., & Mornon, J-P. (1990) *Biochimie 72*, 555–574.
Maggio, M. B., Pagan, J., Parsonage, D., Hatch, L., & Senior, A. E. (1987) *J. Biol. Chem. 262*, 8981–8984.
Mullis, K. B., & Faloona, F. A. (1987) *Methods Enzymol. 155*, 335–350.
Ohta, S., Yohda, M., Ishizuka, M., Hirata, H., Hamamoto, T., Otawara-Hamamoto, Y., Matsuda, K., & Kagawa, Y. (1988) *Biochim. Biophys. Acta 933*, 141–155.
Pai, E. F., Krengel, U., Petsko, G. A., Goody, R., Kabsch, W., & Wittinghofer, A. (1990) *EMBO J. 9*, 2351–2359.
Penefsky, H. S., & Cross, R. L. (1991) *Adv. Enzymol. 64*, 173–214.
Perlin, D. S., Latchney, L., Wise, J., & Senior, A. E. (1984) *Biochemistry 23*, 4998–5003.
Sambrook, J., Fritsch, E. F., & Maniatis, T. (1989). *Molecular Cloning: A Laboratory Manual*, Cold Spring Harbor Laboratory, Cold Spring Harbor, NY.
Saraste, M., Sibbald, P. R., & Wittinghofer, A. (1990) *Trends Biochem. Sci. 15*, 430–434.
Schein, C. (1989) *Bio/Technology 7*, 1141–1149.
Schulz, G. E. (1992) *Curr. Opin. Struct. Biol. 2*, 61–67.
Senior, A. E. (1988) *Physiol. Rev. 68*, 177–231.
Stehle, T., & Schulz, G. E. (1990) *J. Mol. Biol. 211*, 249–254.
Stryer, L. (1978) *Anal. Rev. Biochem. 47*, 819–846.
Stryer, L., & Haugland, R. P. (1967) *Proc. Natl. Acad. Sci. U.S.A. 58*, 719–726.
Tabor, S. (1990) In *Current Protocols in Molecular Biology* (Ausubel, F. A., Brent, R., Kingston, R. E., Moore, D. D., Seidman, J. G., Smith, J. A., & Struhl, K., Eds.) pp 16.2.1–16.2.11, Greene Publishing and Wiley-Interscience, New York.
Tucker, J., Sczakiel, G., Feuerstein, J., John, J., Goody, R. S., & Wittinghofer, A. (1986) *EMBO J. 5*, 1351–1358.
Tybulewicz, V. L. J., Falk, G., & Walker, J. E. (1984) *J. Mol. Biol. 179*, 185–214.
Valencia, A., Chardin, P., Wittinghofer, A., & Sander, C. (1991) *Biochemistry 30*, 4637–4648.
Vignais, P. V., & Lunardi, J. (1985) *Annu. Rev. Biochem. 54*, 917–1024.
Vogel, P. D., Nett, J. H., Sauer, H. E., Schmadel, K., Cross, R. L., & Trommer, W. E. (1992) *J. Biol. Chem. 267*, 11982–11986.
Walker, J. E., Saraste, M., Runswick, M. J., & Gay, N. J.(1982) *EMBO J. 8*, 945–951.
Walker, J. E., Fearnley, I. M., Gay, N. J., Gibson, B. W., Northrop, F. D., Powell, S. J., Runswick, M. J., Saraste, M., & Tybulewicz, V. L. T. (1985) *J. Mol. Biol. 184*, 677–701.
Weber, J., Lee, R. S-F., Wilke-Mounts, S., Grell, E., & Senior, A. E. (1993) *J. Biol. Chem. 268*, 6241–6247.
Wise, J. G., & Senior, A. E. (1985) *Biochemistry 24*, 6949–6954.
Woodward, S. K. A., Eccleston, J. F., & Greeves, M. A. (1991) *Biochemistry 30*, 422–430.
Yohda, M., Ohta, S., Hishabori, T., & Kagawa, Y. (1988) *Biochim. Biophys. Acta 933*, 156–164.
Zhuo, S., Garrod, S., Miller, P., & Allison, W. S. (1992) *J. Biol. Chem. 267*, 12916–12927.